Tunneling spectroscopy of isolated C_{60} molecules in the presence of charging effects

Danny Porath, Yair Levi, Moeen Tarabiah, and Oded Millo*
Racah Institute of Physics, The Hebrew University, Jerusalem 91904, Israel
(Received 24 June 1997)

The discrete molecular-level spectrum of an isolated C_{60} molecule is resolved and its interplay with single-electron charging effects is studied using room-temperature and cryogenic scanning tunneling spectroscopy. The tunneling current-voltage spectra of these molecules exhibit rich structures resulting from both resonant tunneling through the discrete levels and charging effects. In particular, we observe degeneracy lifting within the molecular orbitals, probably due to the Jahn-Teller effect and local electric fields. Theoretical fits account well for our experimental data. [S0163-1829(97)09939-6]

C_{60} molecules were the focus of an intensive study over the last decade and are considered to have many promising future applications.[1] Special effort is directed to electronic molecular level spectroscopy of C_{60}, and in particular to effects that result in shifting and splitting the electronic levels of excited and ionized molecules, such as the Jahn-Teller (JT) distortion.[1,2] At the same time, the interplay between single-electron tunneling (SET) effects and quantum size effects in isolated nano-particles, referred to as ''quantum dots'' (QD), has also gained considerable interest.[3–7] Such an interplay can be experimentally observed most clearly when the charging energy of the dot by a single electron, E_c, is comparable to the electronic level separation ΔE_L, and both energy scales are larger than k_BT. Both effects are relevant to the development of nanoscale electronic devices, such as single-electron (and single-molecule) transistors,[8] and have been studied for various mesoscopic tunnel junction configurations. One example is the double barrier tunnel junction (DBTJ) geometry, where a QD is coupled via two tunnel junctions to two macroscopic electrodes.[3–7] In this system, SET effects, such as the Coulomb blockade (CB) and the Coulomb staircase, can be observed in the current-voltage (I-V) characteristics. The former manifests itself by a suppression of the current around zero bias voltage, while the latter exhibits a sequence of equidistantly spaced steps in the I-V curve.[7]

Our present work combines the two experimental efforts discussed above, namely, we exploit C_{60} molecules as QD's in mesoscopic tunnel junctions and study the interplay between charging effects and resonant tunneling through discrete electronic levels. An isolated C_{60} molecule provides an ideal model system for this research: it is unique due to its size ($\sim$8 Å in diameter), much smaller than the nanoparticles investigated so far, its spherical shape, and its rich electronic spectrum, which is affected by charging. Moreover, this system enables a simultaneous study of the interplay in two regimes, one where the level spacing ΔE_L is larger than E_c (due to molecular orbital spacing), and the other where $\Delta E_L < E_c$ (due to level splitting). Previous works, done on metallic nanoparticles, have treated the case where $\Delta E_L \ll E_c$.[3–7] Due to the above-mentioned properties, an interesting question arises: can one attribute a meaningful effective ''classical'' (geometrical) capacitance to the C_{60} molecule, and describe SET effects in terms of this capacitance? Our data suggest a positive answer.

We have thermally evaporated gold films on glass and annealed them in order to obtain smooth surfaces.[9] C_{60} powder (Aldrich Chem. Co.) was first dissolved in toluene and then transferred to a tungsten boat in a thermal evaporator used only for C_{60}. The solution was allowed to dry and the molecules were deposited onto the substrate. In some samples the evaporation was done directly onto the bare gold film, while in others the gold film was covered by a thin insulating polymethyl-methacrylate (PMMA) layer (less than 40 Å thick, determined by x-ray measurements) before the C_{60} evaporation. The evaporation parameters were adjusted to obtain submonolayer coverage, and, more importantly, isolated molecules, as can be seen in our cryogenic scanning tunneling microscope (STM) images (Fig. 1). In this way we have realized a DBTJ configuration in which a C_{60} molecule is coupled via two tunnel junctions to the gold substrate and the tip of the STM [Fig. 1(a)]. The C_{60} molecules were studied spectroscopically by taking tunneling I-V characteristics, both at room temperature and at 4.2 K.[10] The I-V traces exhibit rich structures due to resonant tunneling through the discrete levels of a C_{60} molecule and charging effects. In addition, they exhibit splitting of degenerate orbitals of the unperturbed molecule due to symmetry breaking that may be caused by charging, external fields, or the JT effect. We note here that in samples where the PMMA layer was not added, most of the molecules exhibited SET and quantum size effects, indicating a large tunneling resistance (compared to the quantum resistance, $h/e^2 \sim 26$ kΩ) for both junctions. The tunnel barrier between the molecule and the gold substrate originates probably from a layer of amorphous carbon and hydrocarbons adsorbed on the gold surface while overheating the boat during evaporation.[10]

The measurement procedure was to first acquire a topographic image and then locate the tip above an isolated C_{60} molecule for the tunneling spectroscopy measurements. For each molecule we have taken I-V curves for different settings of the STM bias voltage V_s and tunneling current I_s and thus for various tip-C_{60} separations. In this way we could change the capacitance C_1 associated with the tip-C_{60} junction [J-1 in Fig. 1(a)] and consequently the ''fractional charge'' Q_0 on the dot and thus the width of the CB.[7,11,12]

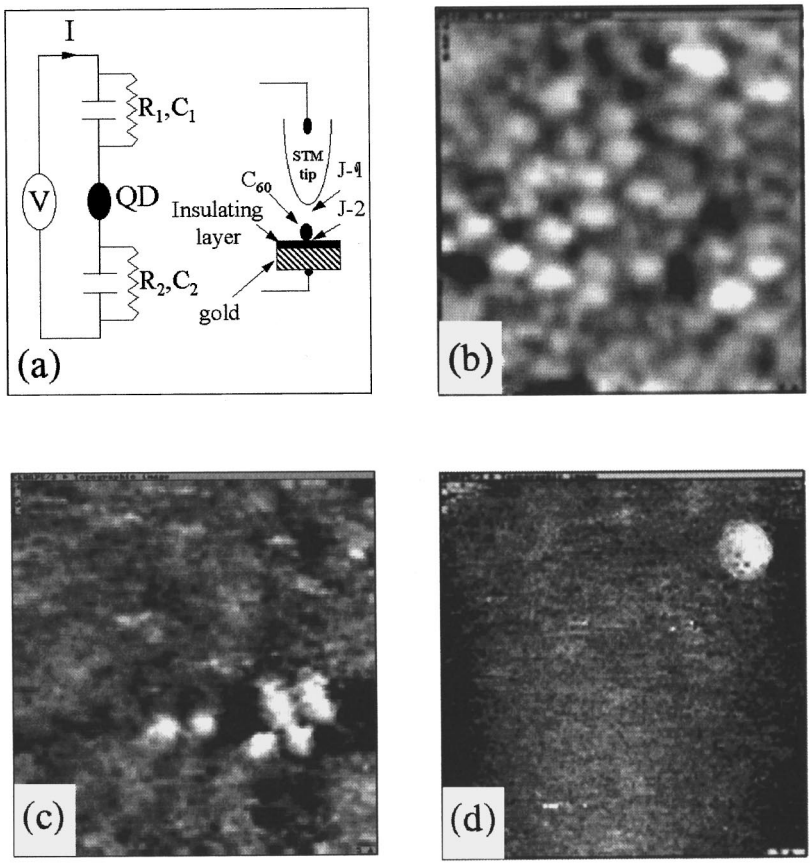

FIG. 1. Schematic and equivalent circuit of the experimental setup: a C_{60} molecule (QD) coupled via two tunnel junctions to the STM tip and gold substrate (a). Three topographic images showing a monolayer of C_{60} (b), a small group of molecules (c), and a single molecule (d), adsorbed on a gold film covered by an insulating layer. The topographic images are of side 70, 100, and 60 Å, respectively. The quality of the background is degraded in comparison to images of bare gold films (Ref. 9), due to the insulating layer.

Each curve was acquired while momentarily disconnecting the feedback circuit, and therefore with constant tip-C_{60} tunnel junction parameters. The I-V measurements were frequently interrupted in order to acquire topographic images and ensure that the tip and the molecule did not drift apart.

In Fig. 2 we plot four I-V characteristics (shifted for clarity) taken for a single molecule at 4.2 K. (Electrons flow from the tip to the substrate for positive bias.) These curves are part of a large set of characteristics acquired with significantly different STM settings. The main features in the I-Vcurves, observed also for many other molecules and samples, are the following: first, there is a *nonvanishing* gap in the curves around zero bias that *oscillates periodically* between minimum and maximum widths as we monotonically change I_s for fixed V_s (and vice versa). This oscillation is due to the periodic variation of $Q_0(\mathrm{mod}\ e)$, consistent with the ''orthodox'' theory and an effective ''classical'' capacitance of the QD. The fact that the minimum gap is *nonzero* indicates that we have an additional contribution, on top of the ''classical'' CB, related to the molecular level spacing. Moreover, in contrast to pure SET characteristics, the curves may get *highly asymmetric* and exhibit steps with *variable widths and heights*. The nearly Ohmic trace shown in the inset was taken in the vicinity of a C_{60} molecule and is typical of the curves obtained everywhere except *over* the molecules. This confirms that the rich structures observed in our data are indeed related exclusively to the C_{60} molecules and not to the PMMA, the carbon layer, or any contaminants on the substrate.

In Fig. 3(a) we plot three experimental I-V characteristics (upper curves) that are part of a set of curves taken with different values of C_1, where in this case $C_1 < C_2$. Below we plot three corresponding theoretical fits (discussed below). It is evident that these curves contain additional steps, beyond those related to SET effects, which reflect the discrete electronic structure of the C_{60} molecule. This structure is exhibited in a more pronounced way in the dI/dV traces, shown in

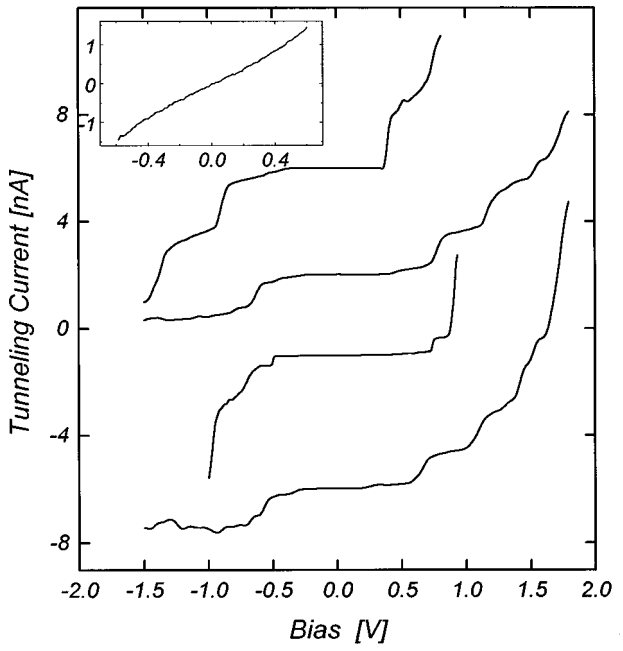

FIG. 2. Tunneling I-V characteristics at 4.2 K taken for a C_{60} molecule in a DBTJ configuration, with different STM settings. Inset: an I-V trace taken near a C_{60} molecule showing Ohmic behavior.

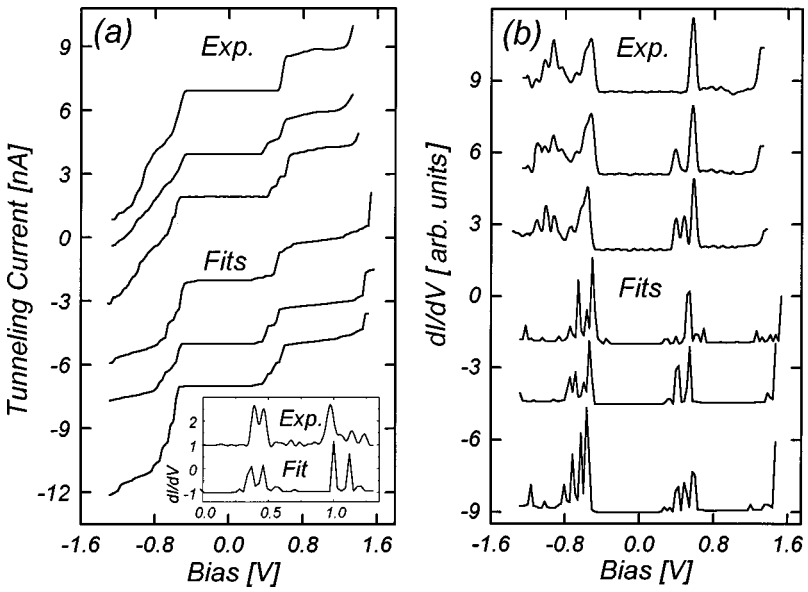

FIG. 3. Tunneling I-V and their dI/dV traces at 4.2 K [(a) and (b), upper curves] and corresponding theoretical fits [(a) and (b), lower curves] for C_{60} in an asymmetric DBTJ ($C_1 < C_2$). Inset: dI/dV curve and fit showing additional group of spectral lines at positive bias.

the inset and in Fig. 3(b), where each peak corresponds to resonant tunneling through a discrete level. Figures 4(b) and 5 are similar to Fig. 3, but taken on other samples and different DBTJ configurations, where $C_1 > C_2$ and $C_1 \sim C_2$, respectively. The effect of the capacitance ratio on the shape of the I-V traces can be clearly seen.

The fits were calculated using the formalism introduced in Ref. 12, which we modified to include the electronic spectrum of C_{60}. The tunneling rate onto the molecule (dot) from electrode $i = 1,2$ is given by

$$\Gamma_i^+(n) = 2\pi/\hbar \int |T_i(E)|^2 D_i(E-E_i) f(E-E_i) D_d(E-E_d) \times [1-f(E-E_d)]dE,$$

where n is the number of excess electrons on the dot. Similar expressions are used for tunneling off the dot, $\Gamma_i^-(n)$. $T_i(E)$ is the tunneling matrix element across junction i. D_i and D_d are the density of states in electrode i and the dot, respectively, E_i (E_d) are the corresponding Fermi levels, whose relative positions *after* tunneling $[E_d(n \pm 1) - E_i(n)]$ depend on n, C_1, C_2, and the level spectrum, and $f(E)$ is the Fermi function. The tunneling matrix elements and the density of states are gathered in the phenomenological ''tunneling resistance'' parameter.[7] However, $T_i(E)$ accounts for the barrier-height dependence on the bias voltage and D_d is taken to be proportional to a set of broadened discrete levels, corresponding to the positions of the electronic energy levels. Following Ref. 12, we first determine the probability distribution of n, $p(n)$, and the tunneling current is calculated self-consistently from

$$I(V) = e\Sigma P(n)[\Gamma_2^+(n) - \Gamma_2^-(n)] = e\Sigma P(n)[\Gamma_1^-(n) - \Gamma_1^+(n)].$$

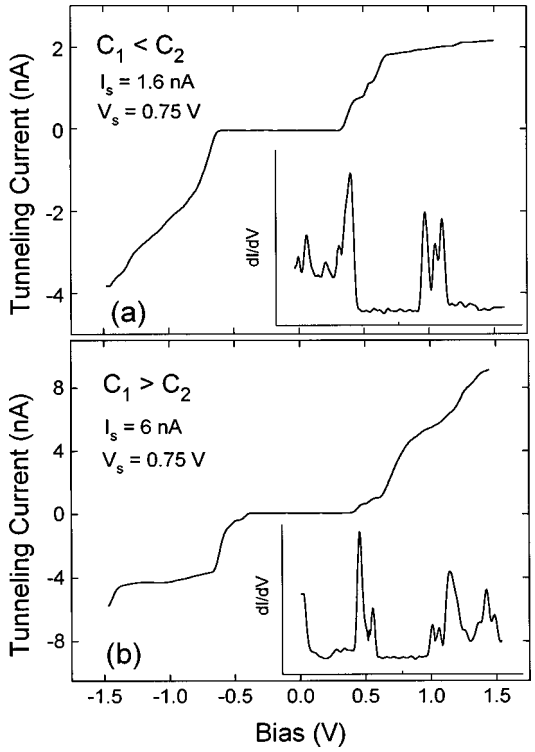

FIG. 4. Tunneling I-V curves obtained for the same molecule, for two different settings, as indicated. In (a) $C_1 < C_2$ and in (b) $C_1 > C_2$. Insets: the corresponding dI/dV traces.

From the fits we obtain information on both the junction parameters and the electronic molecular spectrum. For fitting the energy levels, we have started with theoretical information available for the *neutral* C_{60} molecule, although our data resolve the molecular level structure of *negatively and positively ionized* C_{60}, the possible states of the molecule in the intermediate stage of tunneling through the DBTJ. The molecular level spectrum of the unperturbed, neutral molecule is well understood.[1] The spherical $L = 5$ levels are split into three groups: fivefold degenerate h_{1u} levels, constituting the highest occupied molecular orbital (HOMO), threefold degenerate t_{1u}, the lowest unoccupied molecular orbital (LUMO), and threefold degenerate t_{2u} (LUMO+2). The LUMO+1 (t_{1g}, threefold degenerate) originates from the $L = 6$. These degeneracies can be lifted by several means that

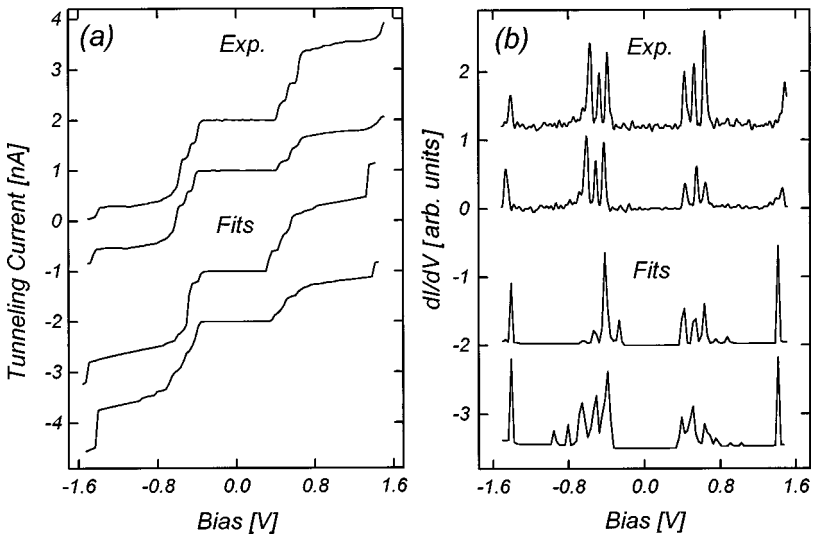

FIG. 5. Tunneling I-V and their dI/dV curves at 4.2 K [(a) and (b), upper curves], and corresponding theoretical fits [(a) and (b), lower curves] for C_{60} in symmetric DBTJ ($C_1 \approx C_2$).

break the icosahedral symmetry. Among these are the following: (1) The electric field between the tip and the substrate and (2) the JT effect, which is prominent in the ionized and excited states of the molecule. Accordingly, we have fitted all our curves using three groups of levels, related to the HOMO, LUMO, and the LUMO+1 orbitals. (The LUMO+2 is too far energetically to be observed in our data). The fits to all our curves (e.g., the sets represented in Figs. 3 and 5) were performed by taking the HOMO levels in the range -0.8 and -0.6 eV, the LUMO in the range 0 to 0.15 eV, and the LUMO+1 onset at ~ 0.6 eV. We note here that the HOMO-LUMO level spacing that we observe, ~ 0.7 eV, is much smaller than the level spacing in the free neutral molecule. It should be pointed out, however, that we are actually measuring the gap between the LUMO(C_{60}^-) and the HOMO(C_{60}^+), since the threshold for tunneling in our DBTJ is determined by the energy of the final, *ionized state*, of the molecule. The typical level splitting that we obtain, ~ 0.05 eV, is somewhat smaller than the predictions for the JT effect.[2]

The electronic wave functions are not isotropic and depend on the spatial location within the molecule. Thus, the tunneling probability to different levels and consequently the I-V characteristics, are sensitive to the *exact* lateral tip position over the molecule, which probably changes slightly from one trace to another within a set. Additional variations among I-V traces may result from different molecular orientations with respect to the substrate. Consequently, the characteristics within a set may show different degrees of level splitting and peak amplitudes (or step heights). In Fig. 3 one can observe a full splitting of the five HOMO levels and the three LUMO levels as well as partially lifted degeneracy of these levels.

We shall now discuss the effect of the junction capacitances on the shapes of the I-V curves. The fits in Fig. 3, excluding the inset, were calculated with $C_1 \sim 0.07$ aF and $C_2 \sim 0.15$ aF, thus $E_c \sim 0.35$ eV. (Both the charging energy and the level separation exceed the thermal energy $k_B T$ even at room temperature, so SET effects and the interplay with the molecular levels can be clearly observed even then.[10]) Since $C_1 < C_2$, tunneling through the DBTJ is onset at junction 1, for the level configuration at hand, where electrons tunnel into the LUMO for positive bias polarity, and off the HOMO for negative bias. [The group at negative bias may also have a small contribution from electrons tunneling onto the LUMO from junction 2.] This is a major source for the pronounced asymmetry observed in the curves. Support for the interpretation above serves the fact that in the opposite case, when $C_1 > C_2$, we obtained I-V curves that are nearly an inversion (with respect to $V=0$) of those in Fig. 3. This is exhibited in Fig. 4, where we plot two I-V curves and their derivatives (insets), obtained for the same molecule. The traces in Fig. 4(a) were taken with $C_1 < C_2$, and those in Fig. 4(b) after reducing the tip-molecule distance to achieve $C_1 > C_2$. Indeed, in the latter the LUMO levels appear at negative bias and the HOMO at positive bias. One should also keep in mind that, as a consequence of the voltage division between the junctions, the real zero bias gaps and molecular level spacings are smaller than those apparent in the I-V curves.

In the inset of Fig. 3 we present a dI/dV curve (and fit) measured for another sample. Here $C_1 \sim 0.13$ aF and $C_2 \sim 0.25$ aF, resulting in a smaller E_c, ~ 0.2 eV. One can now observe, in addition to a doubly split LUMO, another group of three levels, about 0.5 eV to the right of the LUMO. This group can be associated either with the fully split LUMO+1 levels or with a replica of the LUMO group at the onset of the second step of the staircase, i.e., the LUMO(C_{60}^{-2}) levels. It can of course be a combination of the two. The fits to our data suggest that both channels contribute to this group of spectral lines. The onset of this group of levels can also be seen at the right end of other curves.

The traces plotted in Fig. 5(a) are by far more symmetric as compared to those in Figs. 3 and 4. Best fits to these curves (lower two lines) were achieved for $C_1 \approx C_2 \sim 0.15$ aF. In this case tunneling is onset in junction 1 for positive bias and junction 2 for negative bias, through the LUMO levels that are closer to the Fermi energy, according to our fits. Indeed, the dI/dVtraces [Fig. 5(b)] contain groups of three peaks nearly symmetrically positioned around zero bias. At larger voltages the symmetry of the traces should be lost, as the HOMO and the LUMO+1 orbitals will start to contribute.

In summary, we have measured, using STM, the *discrete* tunneling spectra of isolated C_{60} fullerenes in the DBTJ con-

figuration. The spectra manifest the interplay between charging and quantum size effects *simultaneously in two regimes*: $\Delta E_L > E_c$ and $\Delta E_L < E_c$. The degenerate HOMO, LUMO, and possibly the LUMO+1 levels of the unperturbed molecule were split and fully resolved spectroscopically. The degree of splitting is somewhat smaller than predictions for the JT effect. Local fields may contribute to this degeneracy lifting as well. Theoretical curves, calculated using the ''orthodox'' model for SET modified to account for the discrete level spectrum of C_{60}, agree well with our data. The data and the good fits indicate that, in spite of the small size of the molecule, one can associate with it an effective capacitance similar to metallic particles of comparable size, and not in the way suggested in Ref. 13 for atomic size structures. A quantum-mechanical approach is probably more adequate to treat the capacitance in this molecular size regime.

This work was supported by the Israel Academy of Sciences, Grant No. 032-7625.

*Author to whom correspondence should be addressed.

[1] *Fullerenes*, edited by K. M. Kadish and R. S. Ruoff (Electrochemical Society, Pennington, NJ, 1994); C. Joachim, J. K. Gimzewski, R. R. Schlittler, and C. Chavy, Phys. Rev. Lett. **74**, 2102 (1995).

[2] F. Negri, G. Orlandi, and F. Zerbetto, Chem. Phys. Lett. **144**, 31 (1988); N. Koga and K. Morokuma, *ibid.* **196**, 191 (1992).

[3] D. C. Ralph, C. T. Black, and M. Tinkham, Phys. Rev. Lett. **74**, 3241 (1995).

[4] J. G. A. Dubois, J. W. Gerritsen, S. E. Shafranjuk, E. J. G. Boon, G. Schmid, and H. van Kempen, Europhys. Lett. **33**, 279 (1995).

[5] U. Sivan, F. P. Milliken, K. Milkove, S. Rishton, Y. Lee, J. M. Hong, V. Boegly, D. Kern, and M. DeFranza, Europhys. Lett. **25**, 605 (1994).

[6] N. C. van der Vaart, S. F. Godijn, Y. V. Nazarov, C. J. P. M. Harmans, J. E. Mooij, L. W. Molenkamp, and C. J. Foxon, Phys. Rev. Lett. **74**, 4702 (1995).

[7] *Single Charge Tunneling*, edited by H. Grabert and M. H. Devort (Plenum, New York, 1992).

[8] Leo Kouwenhoven, Science **275**, 1896 (1997); M. Bockrath, D. H. Cobden, P. L. McEuen, N. G. Chopra, A. Zettl, A. Thess, and R. E. Smally, *ibid*. **275**, 1922 (1997); S. J. Tans, M. H. Devoret, H. Dai, A. Thess, R. E. Smally, L. J. Geerligs, and C. Dekker, Nature (London) **386**, 474 (1997).

[9] D. Porath, J. I. Gersten, and O. Millo, J. Vac. Sci. Technol. B **14**, 30 (1996).

[10] D. Porath and O. Millo, J. Appl. Phys. **85**, 2241 (1997).

[11] $Q_0 = (C_1 \Delta\Phi_1 - C_2 \Delta\Phi_2)/e$, where the C_i is the capacitance and $\Delta\Phi_i$ is the contact potential across junction $i = 1,2$.

[12] A. E. Hanna and M. Tinkham, Phys. Rev. B **44**, 5919 (1991); E. Bar-Sadeh *et al.*, *ibid*. **50**, 8961 (1994).

[13] G. J. Iafrate, K. Hess, J. B. Krieger, and M. Macucci, Phys. Rev. B **52**, 10 737 (1995).